

**Cell Reports Medicine, Volume 1**

**Supplemental Information**

**A Potential Role for Stress-Induced  
Microbial Alterations in IgA-Associated  
Irritable Bowel Syndrome with Diarrhea**

**Sunaina Rengarajan, Kathryn A. Knoop, Arvind Rengarajan, Jiani N. Chai, Jose G. Grajales-Reyes, Vijay K. Samineni, Emilie V. Russler-Germain, Prabha Ranganathan, Alessio Fasano, Gregory S. Sayuk, Robert W. Gereau IV, Andrew L. Kau, Dan Knights, Purna C. Kashyap, Matthew A. Ciorba, Rodney D. Newberry, and Chyi-Song Hsieh**

**Supplementary Materials for**  
**A potential role for stress-induced microbial alterations in**  
**IgA-associated irritable bowel syndrome with diarrhea**

Sunaina Rengarajan, Kathryn A. Knoop, Arvind Rengarajan, Jiani N. Chai, Jose G. Grajales-Reyes, Vijay K. Samineni, Emilie V. Russler-Germain, Prabha Ranganathan, Alessio Fasano, Gregory S. Sayuk, Robert W. Gereau IV, Andrew L. Kau, Dan Knights, Purna C. Kashyap, Matthew A. Ciorba, Rodney D. Newberry, Chyi-Song Hsieh\*

**Corresponding author. Email: [chsieh@wustl.edu](mailto:chsieh@wustl.edu)**

**The PDF file includes:**

- Figure S1. Immunity and stress, related to Figure 1, 2
- Figure S2. Effects of stress microbiota on germ-free mice, related to Figure 3.
- Figure S3. Dysbiosis induced stress drives immunological alterations, related to Figure 3
- Figure S4. Microbial changes with stress, related to Figure 4.
- Figure S5. IBS-D associated changes in IgA-bound bacteria, related to [Figure 5](#).
- Figure S6. Machine learning prediction of IBS-D, related to Figure 6.
- Figure S7. Clinical characteristics of IgA-associated IBS-D patients, related to Figure 6.
- Table S1. Patient demographics
- Table S2. Infectious colitis history in IBS patients

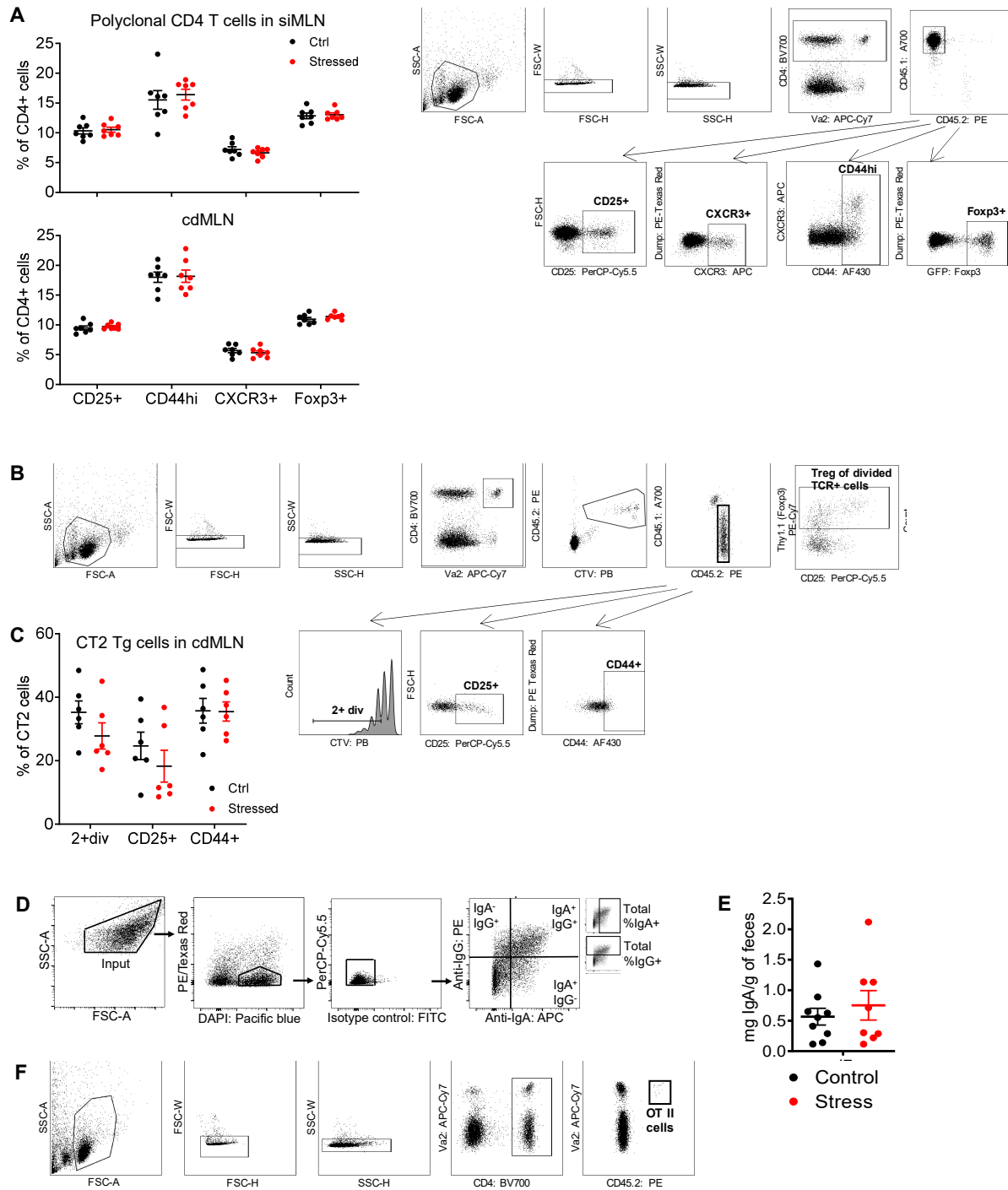


**Figure S1. Immunity and stress, related to Figure 1.** (A) T cell populations with stress. CD4<sup>+</sup> T cell populations were analyzed by flow cytometry on d8 with or without stress as per Figure 1A (left). [Representative schematic](#)

flow-cytometric gating (right). Data shown are gated on host CD4<sup>+</sup> T cells (n=6-8 from 2 experiments). (B) Schematic of flow-cytometric gating for % of Treg of divided transferred congenitally marked naïve CT2 cells, related to Figure 1D. (C) Characterization of transferred CT2 cells with stress, related to Figure 1D (left). Representative schematic of flow cytometric gating of transferred congenitally marked naïve CT2 T cells showing expression of CD25, CD44, and cell division (Cell Trace Violet dilution) (right) (n=6-8 from 2 experiments). (D) Representative schematic of flow-cytometric bacterial sorting with representative IBD specimen. All events that fall within the FSC and SSC gate were sorted as "Input." Bacterial events were gated based on DAPI staining and lack of auto-fluorescence (PerCP-Cy5.5 and PE/Texas Red) and isotype-control antibody staining. Depending on the presence of IgA<sup>+</sup> or IgG<sup>+</sup> events, two to four fractions were sorted from each sample: IgA<sup>-</sup>IgG<sup>-</sup>, IgA<sup>+</sup>IgG<sup>-</sup>, IgA<sup>-</sup>IgG<sup>+</sup> and IgA<sup>+</sup>IgG<sup>+</sup>. (E) Free fecal IgA with stress, related to Figure 1E. One day after the last stress, fecal pellets were washed, spun down, and the concentration of IgA in the supernatant assessed by ELISA (n=8-9 from 2 experiments). (F) Representative schematic of flow-cytometric gating of % of congenitally marked transferred OTII cells of all CD4<sup>+</sup> cells. Data shown are mean +/- S.E.M. and analyzed by Student's t-test.

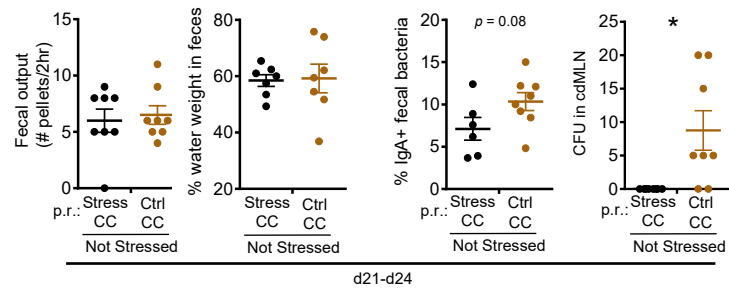


**Figure S2. Effects of stress microbiota on germ-free mice, related to Figure 3.** Bacterial translocation and increased IgA-bound bacteria persist in germ-free mice transplanted with stress microbiota, related to Figure 3C-E. Mice were analyzed at the indicated times after transplant of stressed or control cecal contents (CC) into mice without additional stress (n=6-8 from 2 experiments). Data were analyzed by Student's t-test. \* $P < 0.05$ .

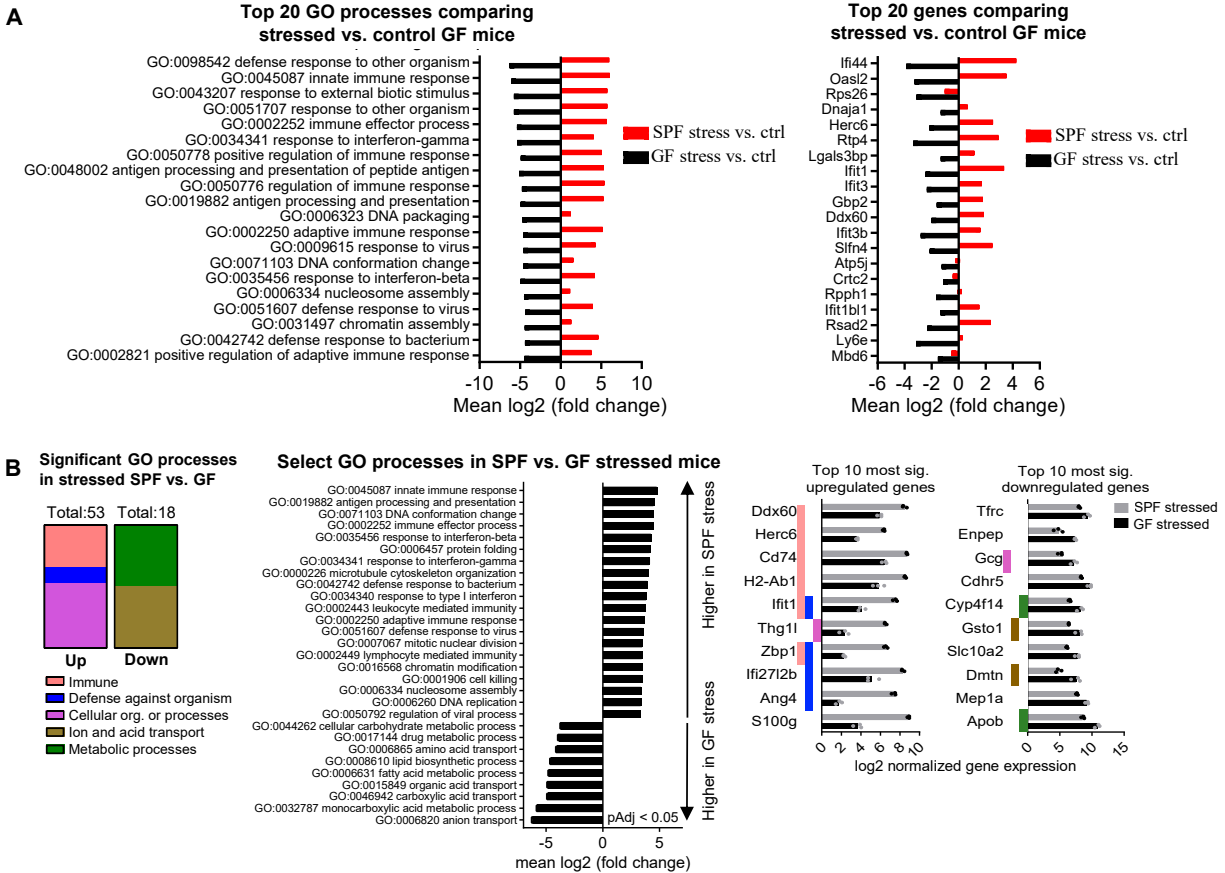


**Figure S3. Dysbiosis induced stress drives immunological alterations, related to Figure 3F.** GF and SPF mice were stressed for 7 days. The following day, the entire colon and cecum with respective un-stressed controls was analyzed by RNA-Seq (n=3/group, 1 expt). (Top) The top 20 Gene Ontology processes or differentially expressed genes by significance (all padj < 0.05) between stressed vs control GF mice are shown as per Figure 3F. (Bottom) All Gene Ontology processes created with Pathview with GAGE padj<0.05 were chosen for display split by the number of upregulated or downregulated processes in SPF stressed vs. GF stressed mice and binned into the displayed general categories (left). Top 10 most significant genes (padj<0.05) that were upregulated or downregulated in SPF stressed vs. GF stressed mice with colors indicating the Gene Ontology processes categories in legend (lower left). All pathways with the category designations and involved gene can be found in Supplementary File 2.

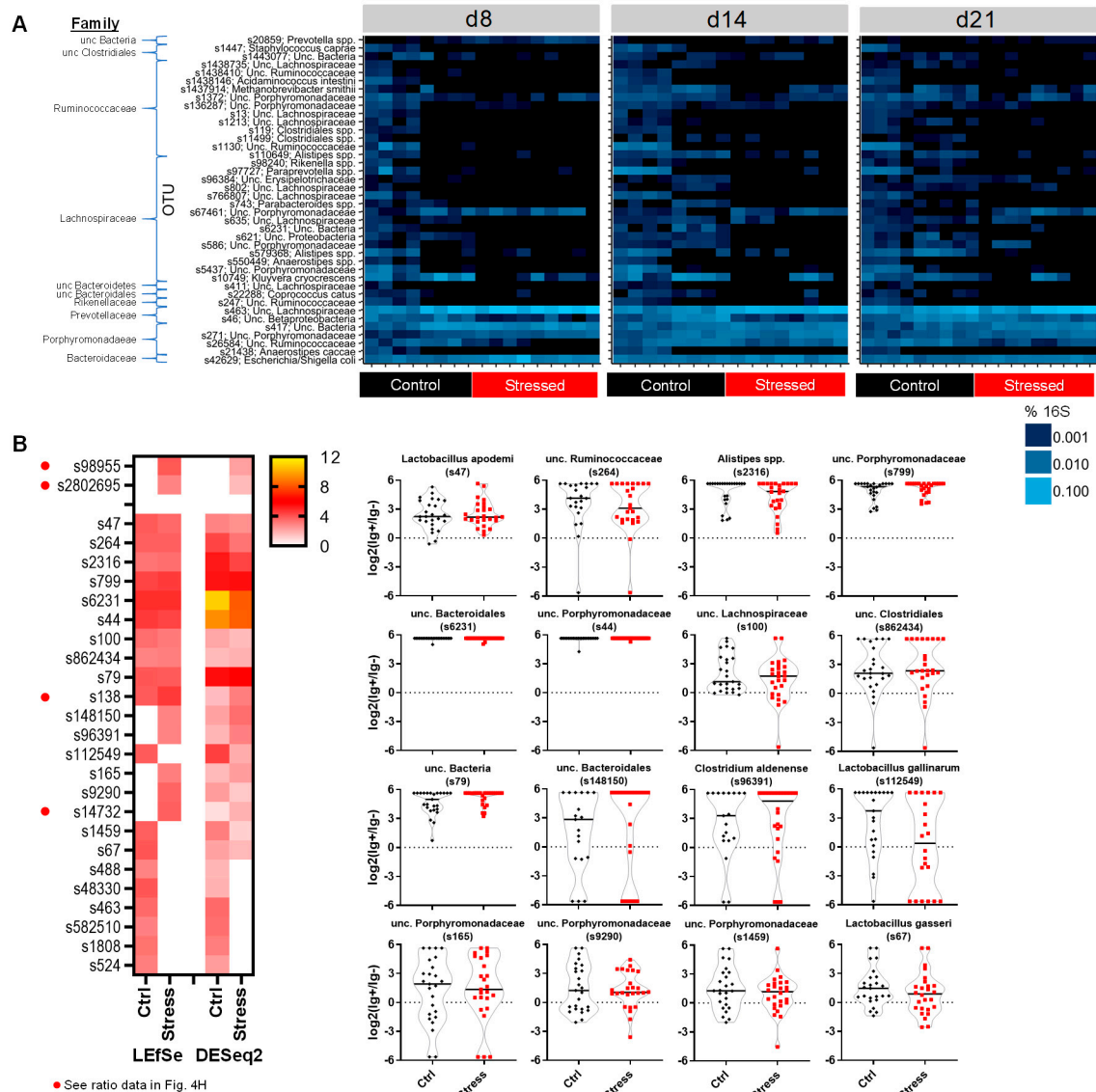


**Figure S4. Microbial changes with stress, related to Figure 4.** (A) Differentially enriched OTUs. Heatmap representation of bacterial frequency changes with stress (Mann Whitney  $U$  padj  $< 0.1$  for all 3 time points), related to Figure 4D-F. Mice were stressed as per Figure 1A and the terminal fecal pellet was analyzed by 16S rRNA sequencing on the indicated days ( $n=8-9$ ). (B) Identification of bacteria increased in the IgA<sup>+</sup> vs IgA<sup>-</sup> fraction. 16S rRNA data were analyzed by DESeq2 and LefSe. The intersection of the OTUs enriched in the IgA<sup>+</sup> fraction in stressed but not control mice are shown as the top 2 OTUs, with the OTUs found IgA-enriched in both stress and control below. OTUs with the red dot are shown in Figure 4H, or otherwise shown on the right. ( $n=24-28$ , pooled d8, d14, d21 data; samples with 0 in IgA<sup>+</sup> and IgA<sup>-</sup> subsets not plotted). Mann Whitney  $U$  test and two to three independent experiments for all panels unless otherwise specified.

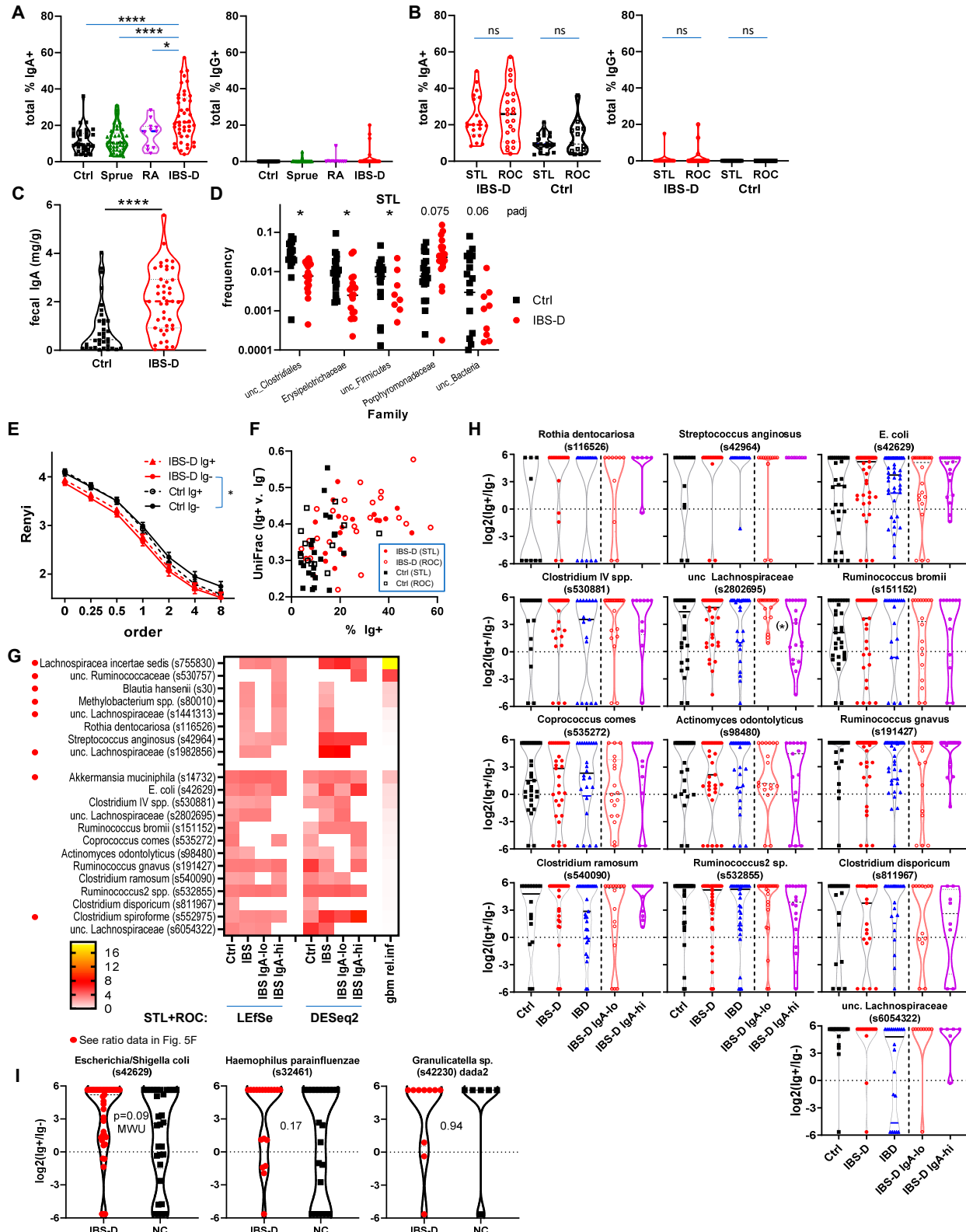


Figure S5. IBS-D associated changes in IgA-bound bacteria, related to Figure 5. (A) IgA-bound bacteria are



not increased in Celiac Sprue or Rheumatoid Arthritis patients, related to Figure 5A. Data were obtained by flow cytometry of fecal samples from RA patients (STL, n=11) or Celiac sprue (Baltimore, n=37). Kruskal Wallis with Dunn's test. (B) Increased IgA-bound bacteria in IBS-D is independent of geography and medical center, related to Figure 5A. Flow cytometry data from fecal samples from STL and ROC were analyzed separately (IBS-D n=20,23; respectively). Student's t-test between STL and ROC samples. (C) Increased free fecal IgA in IBS-D. Fecal samples were diluted in PBS, mixed, and centrifuged. The supernatant was analyzed for IgA by ELISA. Mann Whitney *U* (Ctrl=34, IBS-D=43). (D) Significant changes in microbiota families in IBS-D, related to Figure 5C. Data shown are families that show significant differences between IBS-D and control in STL patients (Mann Whitney *U*, B.H. padj < 0.1, Ctrl=21, IBS-D=20). (E) Alpha diversity of IBS-D IgA+ and IgA- samples. The Renyi entropy was calculated for the indicated data sets. The entropy value reflects diversity; the degree of downward slope with increase order reflects the degree of oligoclonality. Repeated measures ANOVA (Ctrl=34, IBS-D=43). (F) IgA-bound bacteria frequency associated with Unifrac distance between IgA+ and IgA- bacteria, related to Figure 5E (IBS-D n=20 STL, 23 ROC; Ctrl n=21 STL, 13 ROC). (G-H) IgA-enriched OTUs determined by both DESeq2 and LEfSe, related to Figure 5F. The OTUs enriched between IgA+ and IgA- data for both methods are shown in (G). Top OTUs were significant only in IBS-D, whereas bottom OTUs were IgA-enriched in both Ctrl and IBS-D. (H) IgA enrichment of individual OTUs in (G) not shown in Figure 5F. Kruskal Wallis with Dunn's test (Ctrl =34, IBS-D=43, IBD=43, IgA-lo=24, IgA-hi=19). (I) IgA-enrichment of taxa related to Liu et al.<sup>47</sup> Note that *Granulicatella* was found in the dada2 ASVs and not UPARSE OTUs. Mann Whitney *U* *P*-values are shown (Ctrl=34, IBS-D=43). Samples with 0 in IgA+ and IgA- subsets not plotted in (H-I). \**P* < 0.05, \*\*\*\**P* < 0.00005. Each experiment on each patient performed once.

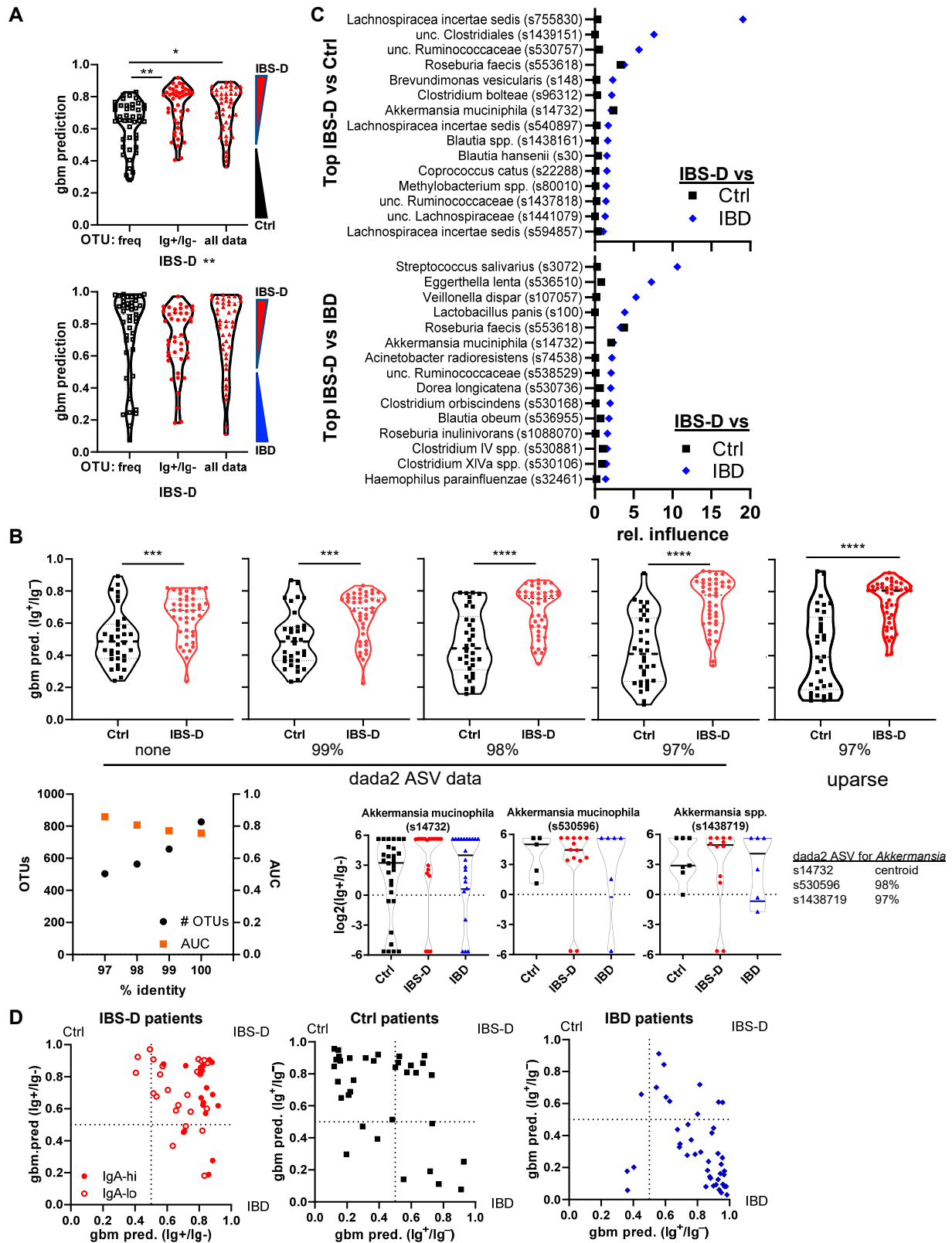
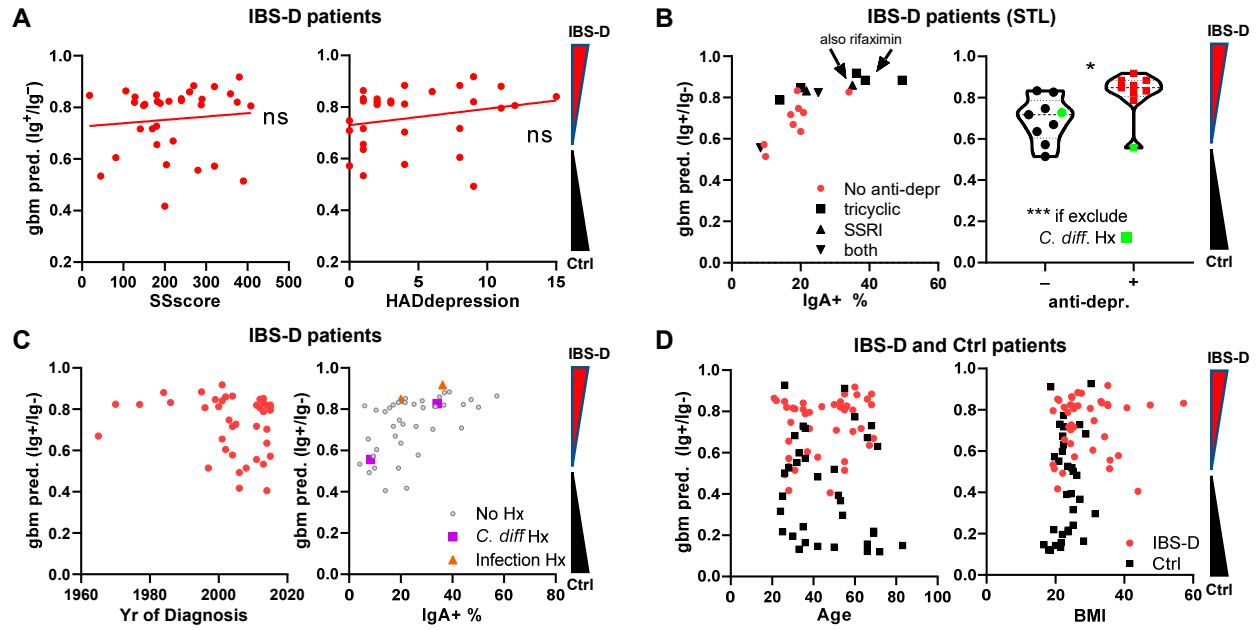


Figure S6. Machine learning prediction of IBS-D, related to Figure 6. (A) Gbm prediction using OTU

frequency, Ig enrichment ratios, or both. Data shown are IBS-D prediction values when modeled against Ctrl or IBS-D as per Figure 6A (contains data from Figure 6A for reference). (B) Gbm prediction using dada2 ASVs. ASVs were also clustered using UPARSE at the indicated percent identity (97-99%) and used for gbm prediction. Data from Figure 6A is shown for direct comparison. The relationship between clustering of ASVs and gbm prediction AUC is shown in the lower left. An example of how ASVs may reduce power compared to clustered OTUs is shown in the lower right for *Akkermansia*. (C) The top 15 OTUs for average relative influence in the gbm models generated between IBS-D vs Ctrl or IBD as per Figure 6A. The average relative influence of the OTU in the other comparison is also shown. (D) Comparison of IBS-D vs Ctrl or IBD gbm prediction values. IBS-D (red), Ctrl (black), or IBD (blue) gbm prediction values (Ctrl=34, IBS-D=43, IBD=43 for all experiments). \* $P < 0.05$ , \*\* $P < 0.005$ , \*\*\* $P < 0.0005$ , \*\*\*\* $P < 0.00005$ . Each experiment on each patient performed once.



**Figure S7. Clinical characteristics of IgA-associated IBS-D patients, related to Figure 6.** (A) Comparison of gbm prediction values with SSscore (STL+ROC, n=14,19) and HADdepression (STL+ROC, n=12,18) values and modeled by linear regression. (B) STL patients on anti-depressants show higher gbm prediction values for IBS-D. (No anti-depr. = 9, tricyclic = 5, SSRI = 2, both = 2; +anti-depr. = 9, -anti-depr.=9). Student's t-test excluding patients with *C. diff.* history (Hx)  $P=0.0004$ , +anti-depr. = 8, -anti-depr.= 8 ( $P=0.02$  if included). (C) No correlation of gbm prediction with duration of diagnosis, n=42 patients returned survey. Gbm prediction and IgA% is shown for infection associated diarrhea, but the low number of cases precludes statistical analysis. (No Hx = 38, *C. diff* Hx = 2, Infection Hx = 2) (D) No correlation of gbm prediction with age or BMI (IBS-D/BMI = 41, IBS-D/Age = 43, Ctrl/BMI = 33, Ctrl/Age = 34). \* $P<0.05$ , \*\*\* $P< 0.0005$ . Each experiment on each patient performed once.

Cohort	Control/Non-IBS		IBS-D		RA	Celiac	IBD
	STL	ROC	STL	ROC	STL	BAL	STL
<b>Number</b>	21	13	20	23	11	37	43
<b>% Female</b>	76.2	76.9	80.0	70.0	90.0	81.1	64.7
<b>Age</b>	53.0 ± 17.5	35.7 ± 11.1	52.1 ± 14.2	38.3 ± 12.6	59.1 ± 12.6	39.7 ± 12.5	45.2 ± 15.7
<b>BMI (n)</b>	21.7 ± 2.7 (20)	25.7 ± 3.3 (13)	30.6 ± 9.3 (17)	27.8 ± 7.5 (23)	27.5 ± 7.4 (11)	N.D.	26.7 ± 6.6 (40)
<b>Race</b>							
% Caucasian	66.7	84.6	100	100	54.5	100	93.0
% African American	19.1	0	0	0	45.5	0	6.9
% Other	14.7	15.4	0	0	0	0	0

**Table S1: Patient demographics, related to Figure 5 and Figure 6**

IBS-D: diarrhea predominant Irritable bowel syndrome.

IBD: Inflammatory bowel disease

N.D.: No data available

Data presented as mean ± S.D.

	<b>Control/NonIBS</b>		<b>IBS-D</b>	
<b>Cohort</b>	STL	ROC	STL	ROC
<b>Infectious colitis<sup>#</sup> history (n (% of total))</b>	0 (0%)	0 (0%)	4 (20%)	0 (0%)

**Table S2: Infectious colitis history in IBS patients**

<sup>#</sup>: Patient endorsed or chart documented history of infectious colitis > 30 days prior to stool specimen collection